Linkages between the circulation and distribution of dissolved organic matter in the White Sea, Arctic Ocean

Pavlov, Alexey K.; Stedmon, Colin A.; Semushin, Andrey V.; Martma, Tõnu; Ivanov, Boris V.; Kowalczuk, Piotr; Granskog, Mats A.

Published in:
Continental Shelf Research

Link to article, DOI:
10.1016/j.csr.2016.03.004

Publication date:
2016

Document Version
Publisher's PDF, also known as Version of record

Continental Shelf Research 119 (2016) 1–13

Contents lists available at ScienceDirect

Continental Shelf Research

journal homepage: www.elsevier.com/locate/csr

Research papers

Linkages between the circulation and distribution of dissolved organic matter in the White Sea, Arctic Ocean

Alexey K. Pavlov [a,b,*,1], Colin A. Stedmon [c], Andrey V. Semushin [d], Tõnu Martma [e], Boris V. Ivanov [b,f], Piotr Kowalczuk [g], Mats A. Granskog [a]

[a] Norwegian Polar Institute, Fram Centre, 9296 Tromsø, Norway
[b] Arctic and Antarctic Research Institute, 199397 Saint Petersburg, Russia
[c] National Institute for Aquatic Resources, Technical University of Denmark, 2920 Charlottenlund, Denmark
[d] Northern Branch of Polar Research Institute of Marine Fisheries and Oceanography (SevPINRO), 163002 Arkhangelsk, Russia
[e] Institute of Geology, Tallinn University of Technology, 19086 Tallinn, Estonia
[f] Saint Petersburg State University, 199178 Saint Petersburg, Russia
[g] Institute of Oceanology, Polish Academy of Sciences, 81-712 Sopot, Poland

ARTICLE INFO

Article history:
Received 28 November 2015
Received in revised form
15 February 2016
Accepted 3 March 2016
Available online 4 March 2016

Keywords:
Colored dissolved organic matter
Dissolved organic carbon
White Sea
Arctic Ocean
Terrestrial runoff

ABSTRACT

The White Sea is a semi-enclosed Arctic marginal sea receiving a significant loading of freshwater (225–231 $km^3\ yr^{-1}$ equaling an annual runoff yield of 2.5 m) and dissolved organic matter (DOM) from river run-off. We report discharge weighed values of stable oxygen isotope ratios ($\delta^{18}O$) of $-14.0‰$ in Northern Dvina river for the period 10 May–12 October 2012. We found a significant linear relationship between salinity (S) and $\delta^{18}O$ ($\delta^{18}O = -17.66 \pm 0.58 + 0.52 \pm 0.02 \times S$; $R^2 = 0.96$, N = 162), which indicates a dominant contribution of river water to the freshwater budget and little influence of sea ice formation or melt. No apparent brine additions from sea-ice formation is evident in the White Sea deep waters as seen from a joint analysis of temperature (T), S, $\delta^{18}O$ and $a_{CDOM}(350)$ data, confirming previous suggestions about strong tidal induced vertical mixing in winter being the likely source of the deep waters. We investigated properties and distribution of colored dissolved organic matter (CDOM) and dissolved organic carbon (DOC) in the White Sea basin and coastal areas in summer. We found contrasting DOM properties in the inflowing Barents Sea waters and White Sea waters influenced by terrestrial runoff. Values of absorption by CDOM at 350 nm ($a_{CDOM}(350)$) and DOC (exceeding 10 m^{-1} and 550 $\mu mol\ l^{-1}$, respectively) in surface waters of the White Sea basin are higher compared to other river-influenced coastal Arctic domains. Linear relationship between S and CDOM absorption, and S and DOC ($DOC = 959.21 \pm 52.99 - 25.80 \pm 1.79 \times S$; $R^2 = 0.85$; N = 154) concentrations suggests conservative mixing of DOM in the White Sea. The strongest linear correlation between CDOM absorption and DOC was found in the ultraviolet ($DOC = 56.31 \pm 2.76 + 9.13 \pm 0.15 \times a_{CDOM}(254)$; $R^2 = 0.99$; N = 155), which provides an easy and robust tool to trace DOC using CDOM absorption measurements as well as remote sensing algorithms. Deviations from this linear relationship in surface waters likely indicate contribution from different rivers along the coast of the White Sea. Characteristics of CDOM further indicate that there is limited removal or change in the DOM pool before it exits to the Barents Sea.

1. Introduction

Arctic rivers are known to supply a substantial load of organic matter to coastal waters (Cooper et al., 2008; Stedmon et al., 2011; Amon et al., 2012), and the terrestrial carbon transported by these rivers plays an important role in the carbon budgets of high-latitude seas (Stein and Macdonald, 2004; Findlay et al., 2015). Due to its light absorbing characteristics, terrigenous DOM entering surface waters of the Arctic Ocean has an impact on upper ocean heating and stratification (Hill, 2008; Granskog et al., 2007, 2015). In addition light absorption by DOM limits light availability for photosynthetic organisms and protects aquatic ecosystem from harmful ultraviolet (UV) radiation (Erickson et al., 2015). The photochemical or microbial mineralization of terrestrial DOM is an

* Corresponding author at: Norwegian Polar Institute, Fram Centre, 9296 Tromsø, Norway.
E-mail address: alexey.pavlov@npolar.no (A.K. Pavlov).
[1] Present address: Norwegian Polar Institute, Fram Centre, Hjalmar Johansens Gate 14, 9296 Tromsø, Norway.

http://dx.doi.org/10.1016/j.csr.2016.03.004
0278-4343/

important and poorly quantified step in the Arctic carbon cycle. The coastal and shelf seas are thought to play a central role in processing terrestrial DOM, with sea ice brine rejection supplying DOM into subsurface (halocline) layers that persist across the Arctic Ocean (Stedmon et al., 2011; Granskog et al., 2012), microbial degradation removing its bioavailable fraction (Helms et al., 2008) and photochemistry further potentially mineralizing DOM in surface waters (Belanger et al., 2006; Xie et al., 2012). Despite this evidence of importance, studies on the fate of DOM in Arctic coastal waters are limited and hindered by remoteness and seasonal accessibility.

The White Sea and its drainage basin in particular have received less attention than other Arctic marginal seas, even though the freshwater received by this shallow marine system considerably exceeds that of other Arctic systems (Filatov et al., 2007). For example, previous studies have reported concentrations of dissolved organic carbon (DOC) in the Northern Dvina river that are three times higher than in other major Siberian rivers (Gordeev et al., 1996, their Table 6). At the same time, some smaller rivers discharging into the north-west White Sea have clear waters (Semushin, Pers. comm.) likely with low DOC, while in some "black rivers" concentrations of DOC may reach up to 5000 μ mol l^{-1} (Pokrovsky et al., 2000). The White Sea is also unique when compared to the rest of the Arctic coastline. It is a large semi-enclosed estuary with a residence time of 1.5–3 years (Filatov et al., 2007), which may contrast with the majority of other rivers that drain directly into the open shelf seas.

The estimated fresh water discharge to White Sea constitutes about 10% of combined discharge from six major Arctic rivers (Ob', Yenisey, Lena, Kolyma, Yukon, and Mackenzie; Cooper et al., 2008). Based on this evidence, we have investigated how the inflow of terrestrial DOM load is distributed in the White Sea system. Here we present results from a sampling initiative to examine the distribution and magnitude of DOM and freshwater in different parts of the White Sea. We report on characteristics and distribution of CDOM, fluorescence of DOM (FDOM), DOC, and their relation to hydrography.

2. Material and methods

2.1. Study area

The White Sea has a surface area of about 90,000 km^2 and receives runoff from a relatively large watershed of 715 000 km^2, resulting in the largest ratio of watershed to sea surface area among all marginal seas of the Arctic Ocean (Filatov et al., 2007). The annual runoff yield for the White Sea is approximately 2.5 m, based on a total annual discharge of about 225–231 km^3 (Filatov et al., 2007). In high discharge years the runoff yield likely exceeds 3 m. This yield is about 8–9 times higher than that of the Arctic Ocean as a whole (Serreze et al., 2006), and 2.5 times greater than that for the Hudson Bay (Granskog et al., 2011), another semi-enclosed Arctic system with high freshwater input. The receiving volume of White Sea, with an average depth of only 67 m (Filatov et al., 2007), is also considerably smaller than the Arctic Ocean or Hudson Bay, emphasizing the potential significance of the large inputs of river water to this marginal sea and further export to adjacent Barents Sea.

Interaction between water masses of the White and Barents seas is controlled by strong tidal mixing in the narrow and relatively shallow Gorlo Strait (Fig. 1), where current velocities of up to 2.5 m s^{-1} have been reported (Filatov et al., 2007). Tidal range significantly varies along the coast of the White Sea, from 1.5 to 2.5 m in the estuaries of the Northern Dvina and Onega rivers, up to 3.5 m in Gorlo Strait, and reaching a maximum up to 10 m in the vicinity of Mezen river mouth. Nearby large rivers outlets (such as the Northern Dvina, Onega and Mezen) as well as at the entrance of Gorlo, distinct hydrographic fronts are typically found (Glukhovskiy, 1991).

Similarly to the Arctic Ocean and Hudson Bay, seasonal sea ice also makes a contribution to the hydrological cycle, although the contribution from sea ice (estimated ice thickness 0.3–0.7 m; Filatov et al., 2007) is not as prominent as in Hudson Bay, where sea ice formation and melt equals or is larger than the freshwater contribution from river water (see Granskog et al. (2011)), or in the Arctic basin, where sea-ice melt is the dominating factor for summer stratification (Peralta-Ferriz and Woodgate, 2015).

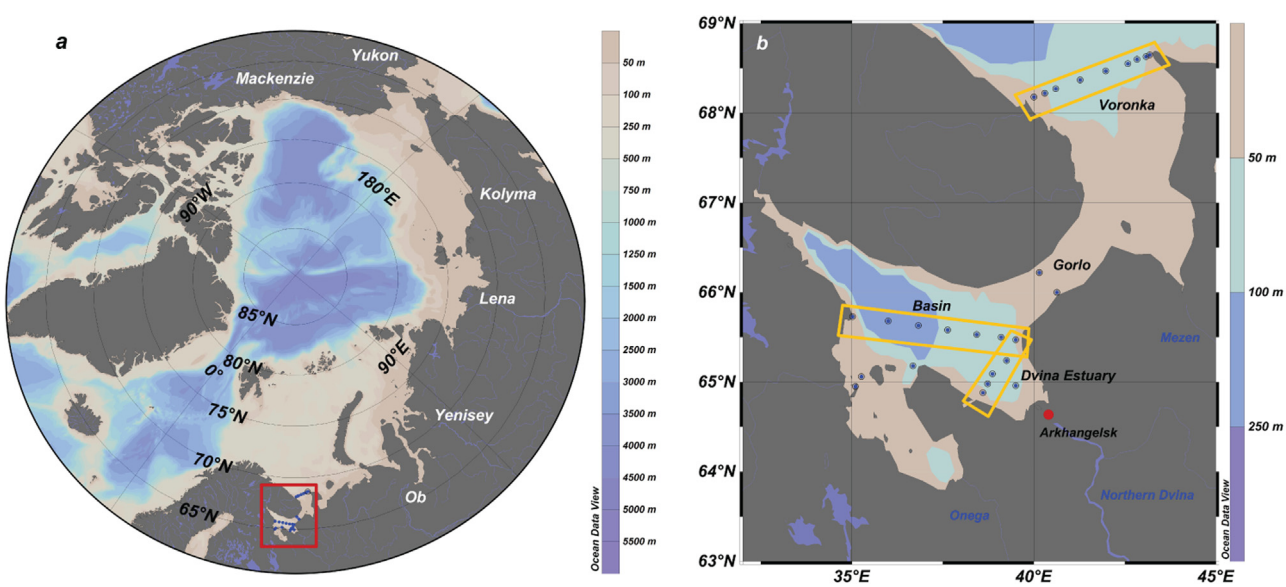

Fig. 1. (a) Location of the White Sea in the Arctic Ocean; (b) sampling sections in the White Sea. The three transects "Voronka", "Basin", and "Dvina Estuary" are highlighted with yellow. These maps were made using the Ocean Data View package (Schlitzer, 2015). (For interpretation of the references to color in this figure legend, the reader is referred to the web version of this article.)

2.2. In situ measurements and sampling

Sampling and hydrographic measurements were performed on three major synoptic sections: across the Northern Dvina estuary, in the main White Sea basin and across the Voronka area at the entrance to the White Sea during «Floating University» cruise onboard RV Professor Molchanov between 28 June and 9 July 2012 (Fig. 1).

In total, 26 stations were visited. At each station, conductivity-temperature-depth (CTD) profiles were made with a calibrated Seabird SBE911plus profiler while seawater samples were collected with SBE32c Compact Carousel water sampler equipped with Niskin bottles. Standard sampling depths included 0, 5, 10, 20, 30, 40, 50, and 75 m with occasional sampling at 15 and 25 m. There were only three stations in the main White Sea basin that had depths exceeding 100 m. On those stations additional samples at 100, 150 and 200 m were collected. Overall, 189 stable oxygen isotope ratio (H_20-$\delta^{18}O$, hereafter $\delta^{18}O$), 156 CDOM and 180 DOC samples were collected. CDOM and DOC samples were collected from Niskin bottles on deck and filtered through pre-rinsed 0.2 μm pore size syringe filters (Pall Acrodisc® PF with Supor® membrane) using all-plastic acid-washed syringes into pre-combusted amber glass vials. Samples were stored in dark and cool until analysis. Water for $\delta^{18}O$ analysis was collected from the same Niskin bottles directly into 15 ml high-density polyethylene bottles, with negligible headspace, and the caps were sealed with Parafilm and kept at room temperature until analysis. For all sampling depths the corresponding temperature and salinity were extracted from the CTD profiles.

2.3. Analytical methods

The CDOM absorbance was measured in the spectral range of 240–600 nm with 3 nm resolution using an Aqualog fluorescence spectrophotometer (Horiba Inc.) and 10 mm quartz cells with fresh Milli-Q water as a blank. Absorbance values were baseline corrected by fitting with the equation following Stedmon et al. (2000), which has a constant, which allows accounting for minor shifts at longer wavelengths. Absorbance values were then converted to an absorption coefficient $a_{CDOM}(\lambda)$ (m^{-1}) following:

$$a_{CDOM}(\lambda) = 2.303 \bullet A(\lambda)/l \quad (1)$$

where A(λ) is the absorbance at a given wavelength λ and l is the path length of the cuvette in meters (here 0.01 m). Absorption spectral slopes were estimated with a non-linear exponential fit (Stedmon and Markager, 2001) for different wavelength ranges, including 300–650 nm, $S_{300-650}$, 350–400 nm, $S_{350-400}$, and 275–295 nm, $S_{275-295}$. Spectral slope ratio, S_R, was calculated after Helms et al. (2008) as $S_{275-295}$:$S_{350-400}$.

DOM fluorescence was measured with an Aqualog fluorescence spectrophotometer (Horiba Inc.) in the excitation range from 240 to 600 nm and emission range from 280 to 620 nm. The raw fluorescence excitation emission spectra were spectrally corrected using factory calibration constants and were corrected for inner filter effects with a method described by Murphy et al. (2010). Corrected spectra were calibrated against the integrated water Raman emission peak excited at 351 nm (Murphy et al., 2010). In this paper we report fluorescence intensities (in Raman units, R.U.) for two traditional DOM fluorescence regions (Coble, 1996): the amino acid-like fluorescence peak T (ex. 276 nm, em. 351 nm) and the humic-like peak C (ex. 351 nm, em. 450 nm). To assess the qualitative transformation of fluorescent DOM we have calculated the ratio of these two fluorescence peaks.

DOC was measured with a Shimadzu TOC-VCPH analyzer using anilide as a standard (Cauwet, 1999) and Consensus Reference Material as a reference (Hansell, 2005). Carbon specific UV absorption also known as SUVA254 (with units of $m^2\,g^{-1}$) was calculated as ratio between CDOM absorption coefficient at 254 nm $a_{CDOM}(254)$ and DOC concentration, following Weishaar et al. (2003) and Murphy et al. (2010).

Samples for $\delta^{18}O$ were analyzed at the Institute of Geology, Tallinn University of Technology, Estonia, using a Picarro L2120-i Isotopic Liquid Water Analyzer with High-Precision Vaporizer A0211. The reproducibility of replicate analysis for the $\delta^{18}O$ measurements was ±0.1‰. The isotope ratios are given in the common delta notation relative to Vienna-Standard Mean Ocean Water (V-SMOW).

2.4. River discharge and oxygen isotope data from Northern Dvina river

Data on river discharge was obtained from the Russian Federal Agency of Water Resources database (https://gmvo.skniivh.ru/), and hydrographs of average daily discharges for the Northern Dvina, Onega and Mezen are shown in Fig. 2. $\delta^{18}O$ samples were collected biweekly from the surface of Northern Dvina (city of Arkhangelsk, 64.53 N, 40.56 E; see Fig. 1) from 10 May to 12 October 2012. Time of sampling coincided with a low tide phase to minimize the potential contribution of seawater from the Northern Dvina estuary. Sampling in the White Sea basin was conducted two months after river discharge peaked in the region (in May) (Fig. 2). Northern Dvina, Onega and Mezen are the major freshwater sources to the White Sea, and two of them (Northern Dvina and Onega) are of particular interest for interpretation of our data on DOM distribution in the White Sea basin.

3. Results

3.1. Freshwater discharge into the White Sea

The Northern Dvina is the major river discharging into the White Sea with an average annual discharge of 108–110 km^3 (Gordeev et al., 1996; Filatov et al., 2007), which is slightly lower than e.g. that of Kolyma and Pechora rivers (Gordeev et al., 1996; Cooper et al., 2008). In 2012, the discharge peaked in early May in the Northern Dvina, Onega and Mezen (Fig. 2). At the mouth of Northern Dvina, values of $\delta^{18}O$ ranged from −15.3‰ in May during spring freshet to −12.0‰ in summer (Fig. 2). Discharge-weighted average of $\delta^{18}O$ in the Northern Dvina between 10 May

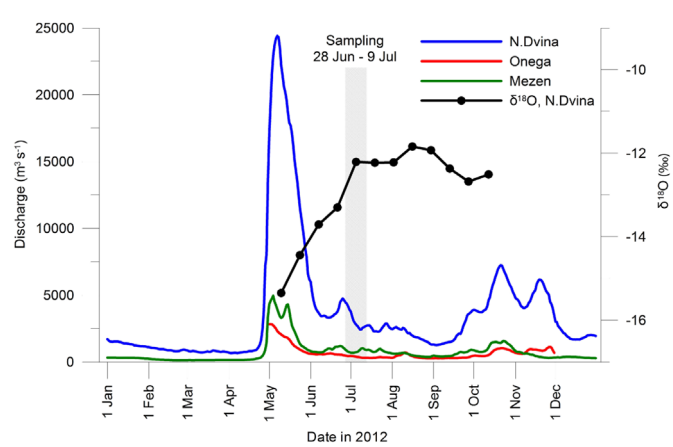

Fig. 2. Average daily discharge from Northern Dvina, Onega and Mezen in 2012. Discharge data is retrieved from a monitoring database of the Russian Federal Agency of Water Resources (https://gmvo.skniivh.ru/). Timing of the White Sea sampling campaign is highlighted with grey shading. Values of $\delta^{18}O$ from freshwater samples collected biweekly in Northern Dvina are also shown.

and 12 October 2012 was −14.0‰. These values are higher than other major Siberian rivers discharging to the Arctic Ocean, and generally fit to the tendency of more negative $\delta^{18}O$ towards the East (Cooper et al., 2008). Riverine values of $\delta^{18}O$ are closest to data from the Ob' river, which is the major Arctic river watershed adjacent to the White Sea basin. Generally, the seasonal cycle of $\delta^{18}O$ in the Northern Dvina is similar to other major Arctic rivers (Cooper et al., 2008) with highest $\delta^{18}O$ values observed in late summer and lowest values observed in spring.

3.2. Hydrography of the White Sea

Distribution of salinity, temperature and $\delta^{18}O$ was investigated on three main hydrographic sections. Along the Voronka section, at White Sea entrance, water masses were relatively uniform and well-mixed except for the north-east part of the section near the coast where warmer waters of lower salinity were found (Fig. 3). Water temperatures ranged between 2.5 and 7.5 °C and salinity ranged between 33.0 and 34.5 across this transect. The Basin

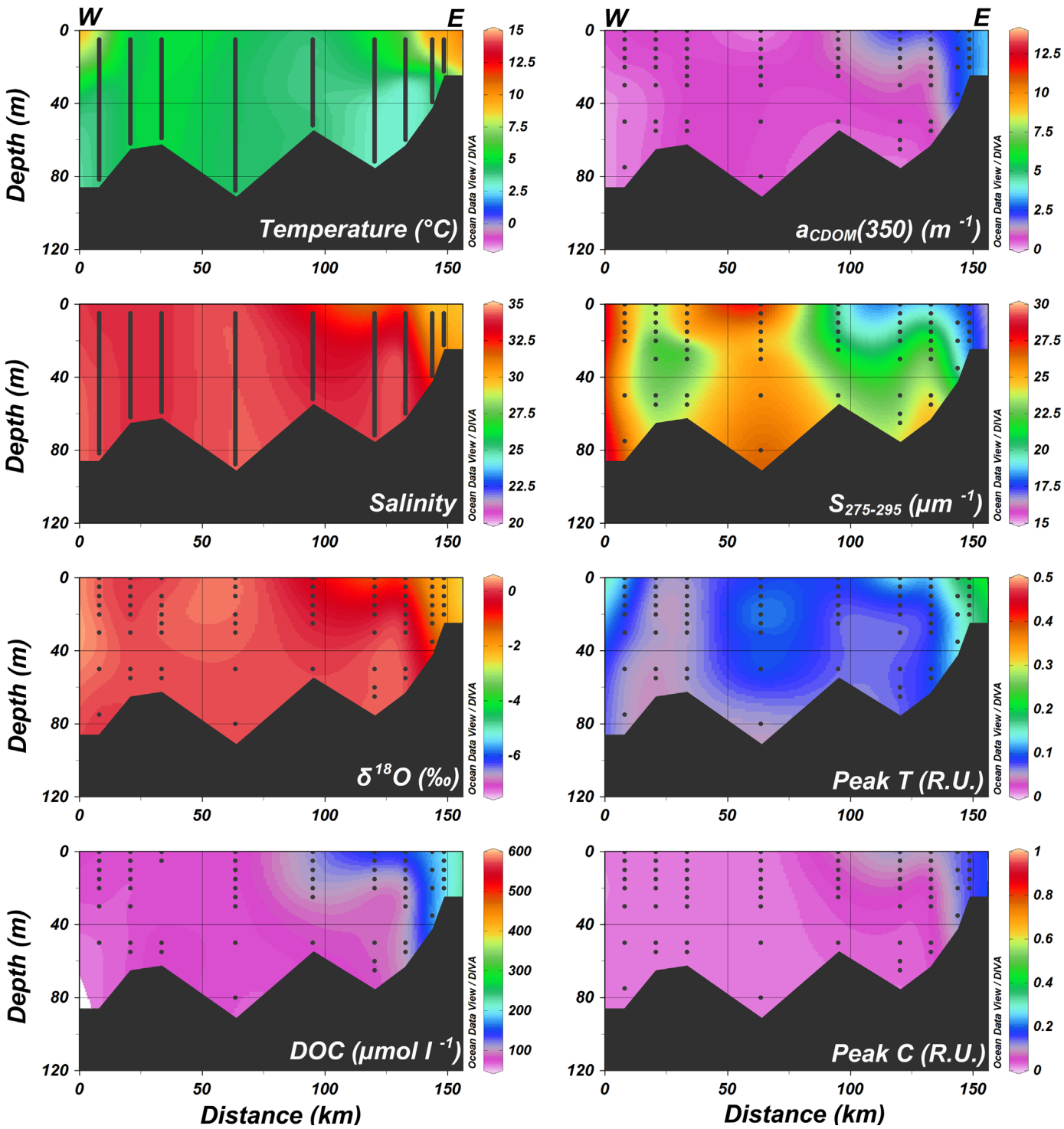

Fig. 3. Distribution of temperature, salinity, stable oxygen isotope ratios, $\delta^{18}O$, dissolved organic carbon, DOC, absorption by CDOM at 350 nm, $a_{CDOM}(350)$ and spectral slope in the range 275–295 nm, $S_{275-295}$, the amino acid-like fluorescence peak T (ex. 276 nm, em. 351 nm) and the humic-like peak C (ex. 351 nm, em. 450 nm), along the "Voronka" section. Note color scale differences of peak T and peak C sections. Zero reference on X-axis is ca. 6 km prior the first station of the section.

section crossed the deepest part of the central White Sea (with depths exceeding 100 m) with sub-zero temperatures from −0.8 to −1.4 °C (temperatures were 0.20–0.25 °C above freezing point) and salinities between 29.2 and 29.9 at depths below 100 m (Fig. 4). A distinct strong vertical stratification was observed along the whole section with a warm and less saline surface layer about 15 m thick, where temperatures ranged between 6 and 12 °C, and salinities between 24.9 and 27.7. The warmest and freshest waters were found in the surface waters of the Dvina Estuary with temperatures up to 15.7 °C and salinity as low as 21.2 (Fig. 5).

Distribution of $\delta^{18}O$ is closely linked to the distribution of salinity and temperature, reflecting the distribution of riverine freshwater and inflowing Barents Sea waters. Lowest $\delta^{18}O$ values of −8.0‰ were observed in the vicinity of the Northern Dvina river (Fig. 5). Barents Sea waters found at Voronka section were characterized by the highest $\delta^{18}O$ values of up to 0.3‰ (Fig. 3). Lowest values in the north-east of the Voronka section indicate outflow of White Sea waters with contribution from river water. A

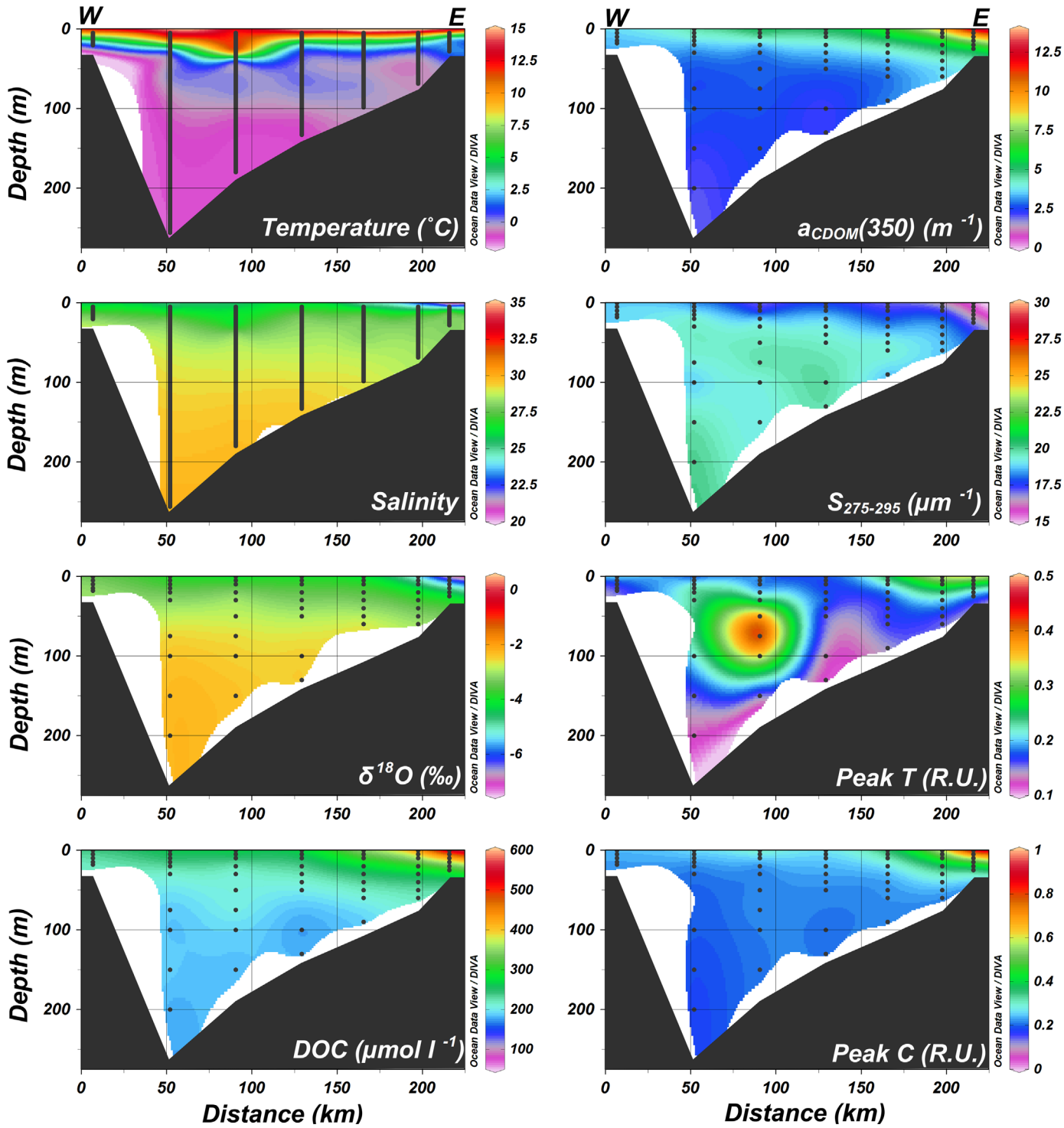

Fig. 4. Distribution of temperature, salinity, stable oxygen isotope ratios, $\delta^{18}O$, dissolved organic carbon, DOC, absorption by CDOM at 350 nm, $a_{CDOM}(350)$ and spectral slope in the range 275–295 nm, $S_{275-295}$, the amino acid-like fluorescence peak T (ex. 276 nm, em. 351 nm) and the humic-like peak C (ex. 351 nm, em. 450 nm) along the "Basin" section. Note color scale differences of peak T and peak C sections. Zero reference on X-axis is ca. 6 km prior the first station of the section.

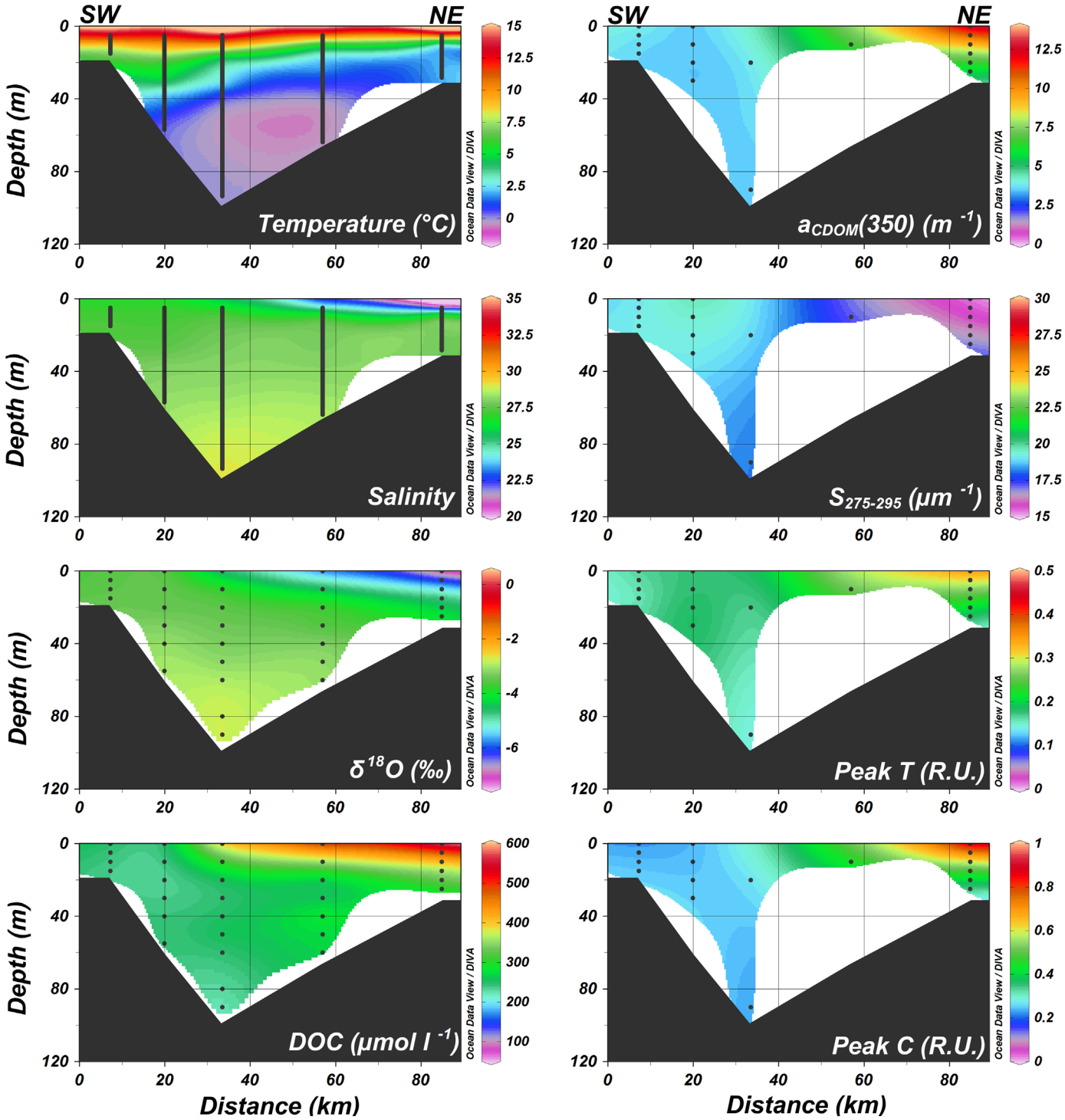

Fig. 5. Distribution of temperature, salinity, stable oxygen isotope ratios, $\delta^{18}O$, dissolved organic carbon, DOC, absorption by CDOM at 350 nm, $a_{CDOM}(350)$ and spectral slope in the range 275–295 nm, $S_{275-295}$, the amino acid-like fluorescence peak T (ex. 276 nm, em. 351 nm) and the humic-like peak C (ex. 351 nm, em. 450 nm), along the "Dvina Estuary" section. Note color scale differences of peak T and peak C sections. Zero reference on X-axis is ca. 6 km prior the first station of the section.

similar pattern was also seen along the Basin and Dvina Estuary section, where lowest $\delta^{18}O$ values were found in the east (Figs. 4 and 5).

3.3. Distribution and properties of DOC, CDOM absorption and fluorescence

Distribution of DOC, CDOM absorption at 350 nm, $a_{CDOM}(350)$, and spectral slope, $S_{275-295}$, follow closely salinity, $\delta^{18}O$, and temperature distributions as seen from all three sections (Figs. 3–5). We found a large variability in $a_{CDOM}(350)$ values, with lowest $a_{CDOM}(350)$ values in the range 0.1–1 m^{-1} found in Barents Sea waters in the western part of Voronka section. Highest $a_{CDOM}(350)$ values, with maximum reaching up to 13.7 m^{-1}, were found in the vicinity of the Northern Dvina estuary in the surface layer. In general, in the uppermost 15 m layer $a_{CDOM}(350)$ gradually decreases from river influenced coastal waters towards the central part of the White Sea. In the central basin, $a_{CDOM}(350)$ values in

subsurface and deeper waters were in the range of 1–3 m^{-1}, which is up to 2–3 times higher compared to Barents Sea waters at the Voronka section.

The spectral slope $S_{275-295}$ ranged from 14.5 to 28.5 μm^{-1} (Figs. 3–5). Largest variability in $S_{275-295}$ was found at the Voronka section. There was a strong spatial gradient from west to east along the Voronka section from 25 $\mu m^{-1} < S_{275-295} < 28.5$ μm^{-1} to 15 $\mu m^{-1} < S_{275-295} < 20$ μm^{-1}. In the White Sea basin and next to Northern Dvina estuary, $S_{275-295}$ was generally in the range of 17–20 μm^{-1}, with lowest values of 14.5–17 μm^{-1} in the proximity of Northern Dvina river.

Lowest DOC values (60–100 $\mu mol\ l^{-1}$) were found in the western and central part of Voronka section within the Barents Sea inflow. Slightly higher DOC concentrations, up to 120 $\mu mol\ l^{-1}$, were measured in the north-east flank of the Voronka section, likely indicating a riverine DOC contribution. Deepest waters in the central Basin had DOC values in the range of 170–190 $\mu mol\ l^{-1}$. Highest DOC concentrations, up to 500 $\mu mol\ l^{-1}$, were found in the vicinity of Northern Dvina estuary. Overall, vertical distribution of DOC follows those of $a_{CDOM}(350)$, T and S, with highest values found in the upper 15–20 m across the White Sea basin.

Spatial distribution of DOM fluorescence was similar to those of $a_{CDOM}(350)$ and DOC. For both, the amino acid-like fluorescence peak T (ex. 276 nm, em. 351 nm) and the humic-like peak C (ex. 351 nm, em. 450 nm), patterns of spatial distribution were generally similar. At Voronka section, peak T ranged from 0.03 to 0.09 (western side of a section) to 0.15–0.23 R.U. (eastern side). At the same time, peak C was between 0.01 and 0.03 and 0.10 and 0.17 R.U. in the western and eastern flanks of the section, respectively. Along the Dvina Estuary section, highest peak T values of up to 0.30-0.35 R.U. were in the surface layer nearby the Northern Dvina, while lowest peak T of 0.13–0.20 R.U. was found in the south-west flank of this section. On the same transect, distribution of peak C showed similar patterns with highest values (0.8–1.0 R.U.) observed next to Northern Dvina and lowest (0.20–0.30 R.U.) on the other side of the section. Along the Basin section, surface waters had peak C values of 0.25–0.3 R.U.in the central and western side, and of 0.8–1.0 R.U. in the east. Deep waters were characterized by peak C below 0.2 R.U. At the same time, highest values of peak T were observed in surface waters nearby the Northern Dvina (0.30–0.35 R.U.) as well as in the central part of transect within a distinct subsurface peak between 50 and 100 m with values reaching 0.4 R.U. Below 100 m, peak T was relatively low down to 0.1.

4. Discussion

4.1. Hydrography and water masses in the White Sea

The White Sea has a complex and dynamic hydrography as several water masses are formed locally as a product of mixing and interaction between external Barents Sea waters and riverine discharge (Glukhovskiy, 1991). Descriptions of summer water masses in the White Sea are sparse but generally distinguish the following waters: Barents Sea water, Gorlo water, surface water of the Basin, intermediate water of the Basin, Deep Water, and freshened surface water in estuaries and bays (Table 1; Glukhovskiy, 1991). With a wide spread in T and S values, ranges encountered during this study do not fit exactly into these classifications (Fig. 6a). Formation of these water masses is closely associated with peculiarities in hydrographic processes across the White Sea throughout the year (Filatov et al., 2007; Glukhovskiy, 1991).

Vertically well-mixed waters found in the central part of Voronka section with temperatures of 4–6 °C and salinities slightly above 34 are close to Barents Sea water that is typically found in Voronka in summer (Fig. 6a). Properties of these waters are close to those described as Barents Sea coastal waters by Loeng (1991).

Sub-surface or intermediate waters found from 40–70 m along the Basin section and some stations on the Dvina Estuary section have temperatures around 0 °C and salinity slightly higher than 28. Spatially, sub-surface waters with sub-zero temperatures in this layer are observed close to Dvina Estuary, while water temperatures above zero are found in the north-west part of the Basin. Previously described as Intermediate water mass of the Basin, these waters are formed through cooling and freshening of Barents Sea waters in a dynamic and relatively shallow Gorlo area in the beginning of winter. Consequently, these waters submerge and spread across the White Sea basin at intermediate depths (Glukhovskiy, 1991).

Similar, but more intense cooling processes in Gorlo towards the end of winter and in the beginning of spring are responsible for a formation of the Deep Water, found below 100 m in the central part of the Basin section (Glukhovskiy, 1991; Filatov et al., 2007). These water masses are uniform and have core temperature and salinity of −1.4 °C and 29.7, respectively (Fig. 6a). Formation of Deep Water provides a regular mechanism for water mass exchange and ventilation in the deep central White Sea basin (Glukhovskiy, 1991). These waters were found to be 0.20–0.25 °C above freezing point (Fig. 6b), and thus it appears that sea ice formation has a minor role in the vertical mixing in the White Sea, neither does the isotopic composition (Fig. 4) point to any significant brine additions to the deep waters, in contrast to Hudson Bay (Granskog et al., 2011) and Arctic shelf seas (Bauch et al., 2009). Likely the significant buoyancy from freshwater inputs limits deep convection by brine release from sea ice formation.

A warm and relatively fresh upper layer of about 5 m found in the vicinity of the Onega and Northern Dvina river mouths is a typical feature observed in summer, and especially pronounced in the absence of wave-induced mixing. These waters have previously been named as a Fresh water of estuaries and bays (Glukhovskiy, 1991). Spreading further towards the central basin this water mass

Table 1
Water masses found in the White Sea in summer (after Glukhovskiy (1991)).

Water mass	TS properties	Location	Remarks
Deep water (DW)	$T_{core} = -1.4$ °C; $S_{core} = 29.7$	Basin	Homogeneous below 100 m. Source: Barents Sea waters cooled and freshened in Gorlo in the end of winter and beginning of spring.
Barents Sea water (BSW)	$T_{core} = 5.7$ °C; $S_{core} = 34.16$	Voronka	Vertically homogeneous in summer.
Intermediate water of the Basin (IW)	$-0.2 < T < 0.9$ °C; $28.0 < S < 28.2$	Basin	Found between ca. 40 and 70 m. Source: Barents Sea waters cooled and freshened in Gorlo in the beginning of winter.
Gorlo water (GW)	$5.96 < T < 6.85$ °C; $27.83 < S < 28.42$	Gorlo	Homogenous due to strong tidal mixing.
Surface water of the Basin (SWB)	$10.0 < T < 12.0$ °C; $25.9 < S < 27.0$	Basin	Warm and relatively fresh upper layer of ca. 20 m.
Fresh water of estuaries and bays (SWEB)	T of up to 16.1 °C; S of down to 21.2–23.0	Estuaries and coastal areas	Warm and relatively fresh upper layer of 5 m.

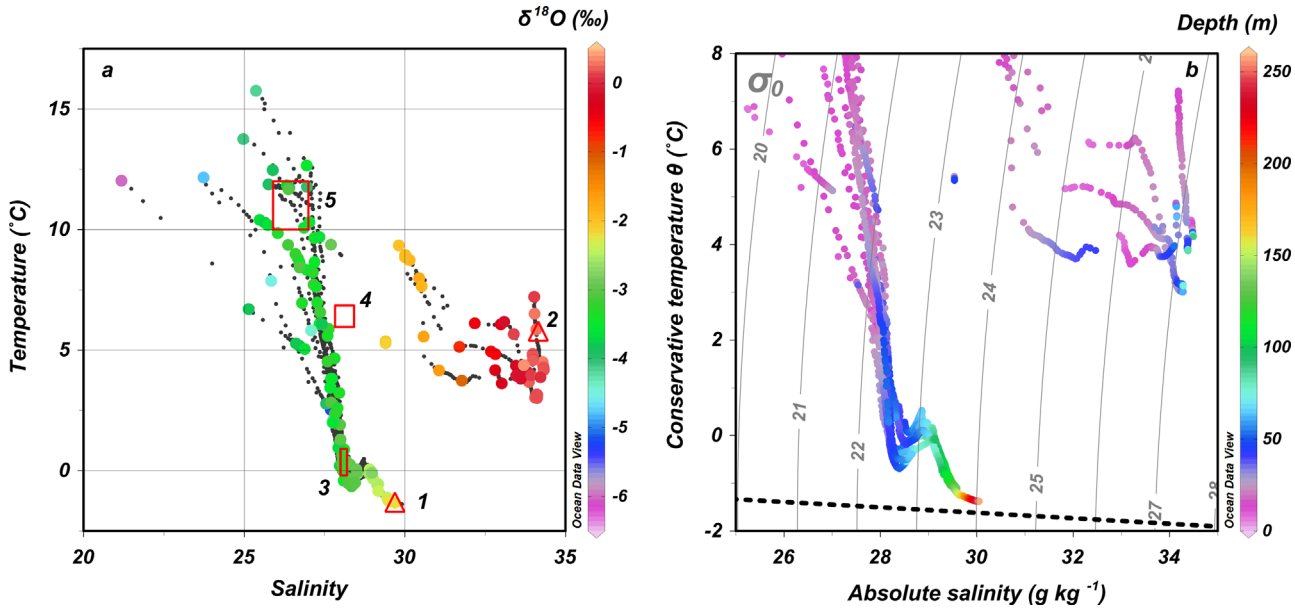

Fig. 6. (a) Temperature – Salinity plot with stable oxygen ratio ($\delta^{18}O$) as the third variable. Numbers indicate either core TS properties or ranges of following water masses (see text, and Table 1): Deep water (1), Barents Sea water (2), Intermediate water (3), Gorlo water (4), Surface water of the Basin (5); (b) Conservative temperature – absolute salinity plot with color scale showing depth. Isopycnals are shown by grey lines (reference pressure is 0 dbar). Dotted line indicates the freezing temperature as a function of absolute salinity (reference pressure is 0 dbar). Conservative temperature and absolute salinity were calculated based on TEOS-10 (McDougall and Barker, 2011).

is confined to the uppermost layer and is further mixed with underlying waters, thus creating a thicker mixed layer of about 20 m depth with typical S of 25.9–27.0, and T of 10–12 °C, though as seen in our study T-S properties are not limited to these ranges. These waters are ubiquitous in the White Sea proper and typically referred as a Surface water of the Basin (Glukhovskiy, 1991).

$\delta^{18}O$ and its relation to water masses support the description of the hydrography based on temperature and salinity. Barents Sea waters found at the Voronka section were characterized by highest salinity and $\delta^{18}O$ values (up to 34.3 and 0.3‰, respectively). These $\delta^{18}O$ values are comparable to upstream Atlantic waters (Bauch et al., 2009; Dodd et al., 2012). Deep and intermediate water masses have $\delta^{18}O$ of -2 to -4‰ and essentially lie on the mixing line between Barents Sea waters and river-influenced waters of estuaries and bays that have $\delta^{18}O$ of down to -8.0‰, which indicates that their formation was associated with a mixing of Barents Sea waters and freshened waters of the White Sea. This resembles the Hudson Bay (Granskog et al., 2011), in the fact that some of the river runoff is carried during winter cooling all the way to the bottom of the deep basin. Thus vertical mixing is also a component of the freshwater cycling in the White Sea, and it is apparent that strong tidal mixing in Gorlo area is at least locally able to penetrate the strong surface stratification that builds up in summer. On the other hand, contrary to Hudson Bay, no sign of significant brine additions from sea-ice formation is evident in the White Sea deep waters, which indicates that sea ice does not play a significant role in deep water formation of freshwater inputs to the deep waters in the White Sea.

4.2. Distribution of DOC and CDOM in the White Sea

Observed $a_{CDOM}(350)$ values in the Barents Sea waters across Voronka section were generally higher than those found within Atlantic waters in the Central Barents Sea and in the Fram Strait (Hancke et al., 2014; Pavlov et al., 2015), which has been shown to be predominantly of marine origin in summer time (Hancke et al., 2014). The lower salinity water observed along Voronka section had elevated $a_{CDOM}(350)$ compared to the central Barents Sea and this indicates a contribution of terrestrial CDOM from the White Sea to the adjacent Barents Sea and the Arctic Ocean shelf (Fig. 3). DOC values of 60–100 μmol l^{-1} were within the range of DOC in upstream Atlantic waters in the Norwegian Sea, which was reported between 53 and 149 μmol l^{-1} (Bøsrheim and Myklestad, 1997), comparable to Kongsfjorden, Svalbard with reported DOC in the range of 70–115 μmol l^{-1} (Pavlov et al., 2014), and exceed DOC concentrations of 52 ± 4 μmol l^{-1} found in the upper 150 m in the St. Anna Through in northern Barents Sea (Fransson et al., 2001).

Observed $a_{CDOM}(350)$ and DOC values in the deep waters in the central White Sea were higher than $a_{CDOM}(350)$ and DOC values found in the Barents Sea waters in Voronka (Figs. 3 and 4). The White Sea deep waters are formed in winter and spring as a result of cooling of Barents Sea water mixing with waters exiting White Sea in Gorlo (Glukhovskiy, 1991; see also Section 4.1). Therefore, elevated $a_{CDOM}(350)$ and DOC values in deeper waters are explained by the contribution of terrigenous organic material in line with the waters having an isotopic signature from river waters.

Highest values of $a_{CDOM}(350)$ and DOC in the upper layer were associated with waters with lower salinity influenced by riverine runoff. These values are lower compared to CDOM absorption and DOC concentrations in rivers discharging into the Arctic Ocean (Cooper et al., 2008; Stedmon et al., 2011), but significantly higher than those found in the coastal waters of Siberian and North American shelf seas (Kattner et al., 1999) or Hudson Bay (Granskog et al., 2007). Regression against salinity gives a zero-salinity $a_{CDOM}(350)$ of 18.8 ± 1.6 m^{-1} and DOC of 959 ± 53 μmol l^{-1}, which are among the highest flow-weighed CDOM and DOC concentrations among major Arctic rivers (Lobbes et al., 2000; Cooper et al., 2008; Alling et al., 2010; Stedmon et al., 2011). This agrees with the previous findings from Northern Dvina river by Gordeev et al. (1996), who reported even higher average annual DOC concentrations of up to 20.1 mg l^{-1} (corresponding to 1675 μmol l^{-1}). Apart from Northern Dvina, the largest river in the White Sea basin, some smaller rivers have been reported to have DOC concentrations of up to 60 mg l^{-1} (5000 μmol l^{-1}) (Pokrovsky et al., 2000).

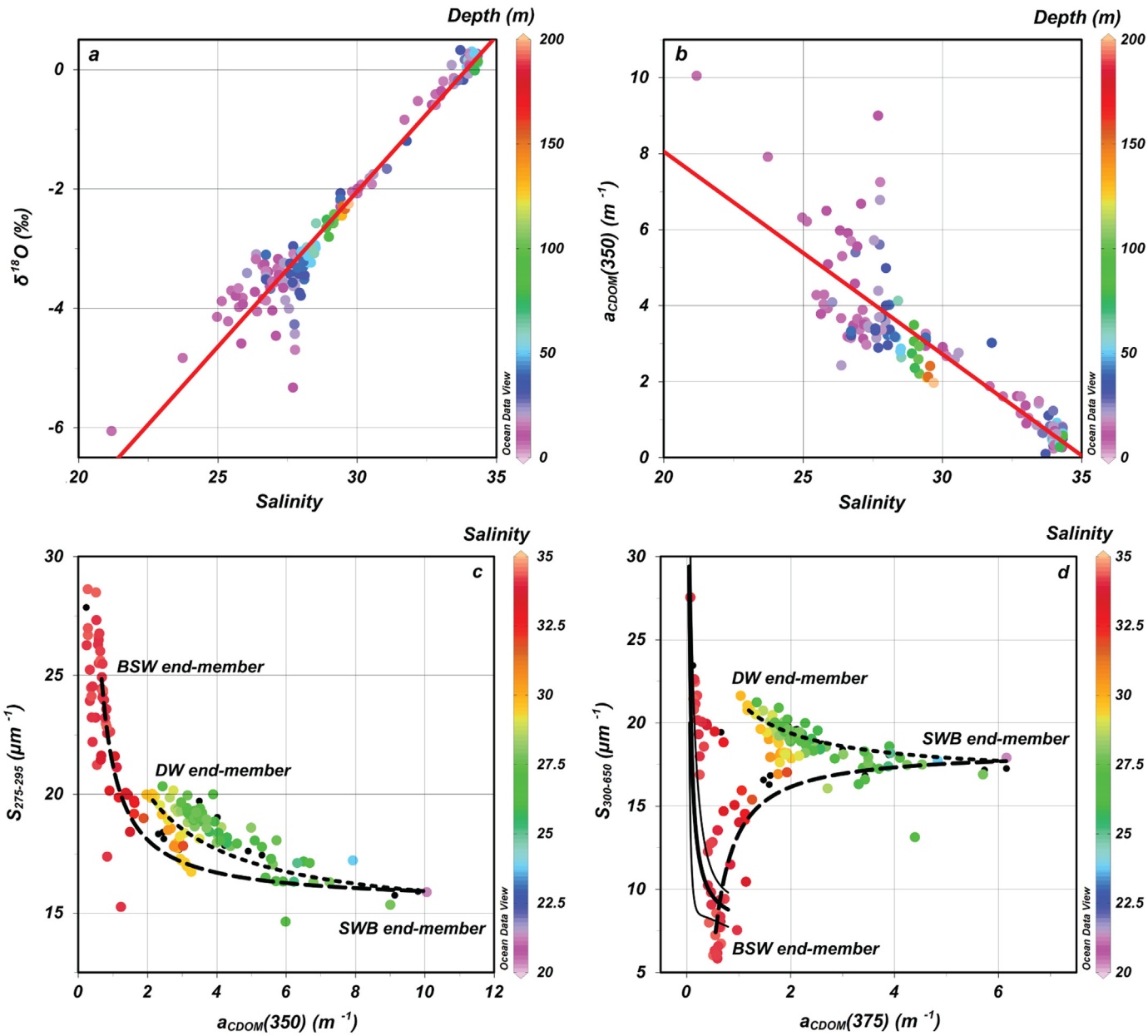

Fig. 7. Property-property plots of following variables: (a) stable oxygen ratio ($\delta^{18}O$) – Salinity, color scale – CDOM absorption at 350 nm, $a_{CDOM}(350)$; (b) $a_{CDOM}(350)$ – Salinity, color scale – $\delta^{18}O$; (c) $S_{275-295} - a_{CDOM}(350)$, color scale – Salinity; (d) $S_{300-650} - a_{CDOM}(375)$, color scale – Salinity. In panel (d) thick solid line shows the marine CDOM relationship from Stedmon and Markager (2001), while thin solid lines show the model limits. Black dots on all figures represent points with missing 3rd variable data (color scale). On plots (c) and (d) theoretical conservative mixing lines between surface water of the Basin (SWB) and Barents Sea water (BSW), and Surface water of the Basin (SWB) and Deep water (DW) are shown with a dashed and dotted lines, respectively. Both lines are calculated after Stedmon and Markager (2003). For plots (a) and (b), linear fits are shown with corresponding statistics in Table 2.

4.3. Properties of DOM and relationship to hydrographic variables

The linear relationship between salinity and $\delta^{18}O$ is significant (Fig. 7a, Table 2) and this is somewhat expected in a region heavily influenced by riverine runoff which by far exceeds the contribution of freshwater from sea-ice melt. Deviations from a straight line occur in the surface layer likely indicating different freshwater end-members. The linear regression gives a zero-salinity $\delta^{18}O$ value (intercept) of -17.7 ± 0.6‰ (Table 2), which is lower than $\delta^{18}O$ measured in the Northern Dvina river during the summer season of 2012 (between -11.8 and -15.3‰). The minimum $\delta^{18}O$ of -15.3‰ in Northern Dvina was observed on May 10th, the first date of sampling when majority of the annual discharge occurs. It is possible that lower $\delta^{18}O$ would be found earlier in spring

Table 2
Relationships between hydrographic variables, absorption by CDOM at different wavelengths, DOC concentration, specific CDOM absorption and spectral slopes. α and β are regression coefficients (intercept and slope) with corresponding 95% confidence intervals. R^2 is a coefficient of determination and N is number of data points.

	Equation	α	β	R^2	N
1	$\delta^{18}O = \alpha + \beta \cdot S$	-17.66 ± 0.58	0.52 ± 0.02	0.96	162
2	$DOC = \alpha + \beta \cdot S$	959.21 ± 52.99	-25.80 ± 1.79	0.85	154
3	$a_{CDOM}(350) = \alpha + \beta \cdot S$	18.81 ± 1.56	-0.54 ± 0.05	0.77	142
4	$a_{CDOM}(375) = \alpha + \beta \cdot S$	11.14 ± 1.07	-0.32 ± 0.03	0.71	142
5	$DOC = \alpha + \beta \cdot a_{CDOM}(350)$	70.03 ± 5.67	40.60 ± 1.48	0.96	155
6	$DOC = \alpha + \beta \cdot a_{CDOM}(300)$	65.39 ± 3.64	17.30 ± 0.40	0.98	155
7	$DOC = \alpha + \beta \cdot a_{CDOM}(254)$	56.31 ± 2.76	9.13 ± 0.15	0.99	155

especially with earlier snow melt in the season, however observations from other major Siberian rivers indicate that lowest $\delta^{18}O$ do typically occur in May (Cooper et al., 2008), while the peak discharge occurs in June (Stedmon et al., 2011). One needs to take into account that we consider all samples collected across the White Sea and $\delta^{18}O$ values might differ in rivers other than the Northern Dvina, which accounts for slightly less than 50% of the total discharge to the White Sea (Filatov et al., 2007).

CDOM absorption $a_{CDOM}(350)$ shows an increase with decreasing salinity (Fig. 7b). Such relationships have been widely used in tracer studies in order to understand the fate and transformation processes of terrigenous DOM (CDOM) in the Arctic Ocean (Cauwet and Sidorov, 1996; Granskog et al., 2007, 2012; Anderson and Amon, 2014; Stedmon et al., 2015). In this study, a nearly linear relationship was found between salinity and $a_{CDOM}(350)$ (as well as $a_{CDOM}(375)$) (Table 2, Fig. 7b). Deviations at salinity below 28 can be attributed to apparent differences in CDOM signals between Onega and Northern Dvina rivers (not shown) as well as by a contribution from smaller rivers along the White Sea coast. Therefore, a more detailed spatial and temporal survey would help to refine the relationship between salinity against CDOM absorption. Deepest samples (> 150 m, as indicated by color scale on Fig. 7b) lie on the mixing line between more saline Barents Sea waters and waters influenced by river run off, which is again consistent with previous suggestions about mechanisms responsible for the formation of deep and intermediate waters in the White Sea basin, by mixing in Gorlo Strait in spring and winter (Glukhovskiy, 1991).

Fig. 7c,d demonstrate the relationship between spectral slope $S_{275-295}$ and $a_{CDOM}(350)$, and $S_{300-650}$ and $a_{CDOM}(375)$. The latter has been previously used to differentiate characteristics of marine CDOM (Stedmon and Markager, 2001). Generally, in the transition

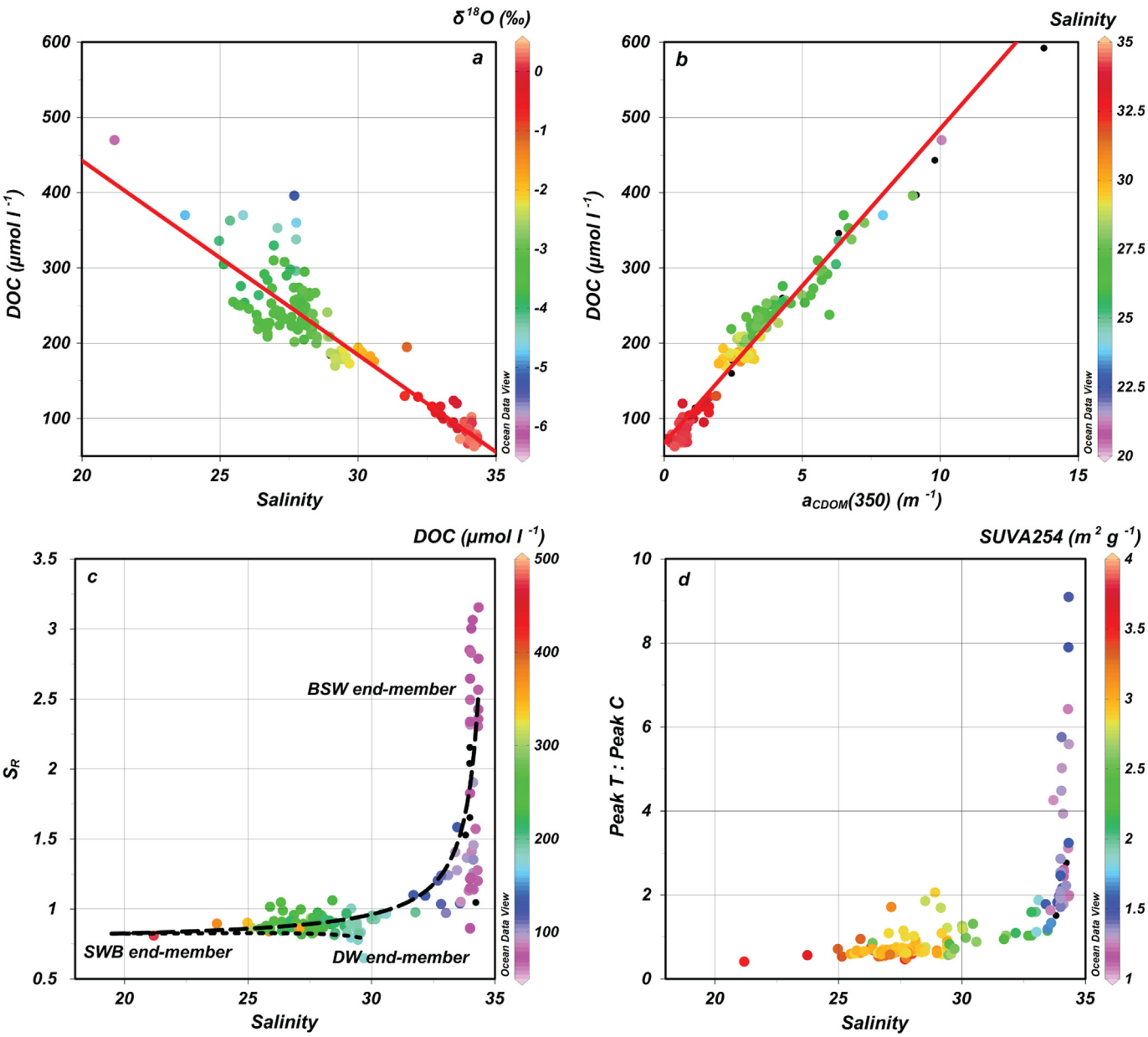

Fig. 8. Property-property plots of following variables: (a) dissolved organic carbon (DOC) – Salinity, color scale – stable oxygen ratio ($\delta^{18}O$); (b) DOC – CDOM absorption at 350 nm ($a_{CDOM}(350)$), color scale – Salinity; (c) spectral slope ratio S_R ($S_{275-295}$:$S_{350-400}$) – Salinity, color scale – DOC; Black dots on all figures represent points with missing 3rd variable data (color scale); (d) Fluorescence intensity ratio (Peak T:Peak C) – Salinity, color scale – SUVA254. On plot (c) theoretical conservative mixing lines between Surface water of the Basin (SWB) and Barents Sea water (BSW), and Surface water of the Basin (SWB) and Deep water (DW) are shown with a dashed and dotted lines, respectively. Both lines are calculated after Stedmon and Markager (2003). For plots (a) and (b), linear fits are shown with corresponding statistics in a Table 2.

from terrestrial to marine and oceanic environments the spectral slope increases with decreasing CDOM absorption (Blough and Del Vecchio, 2002). The nonlinear relationship between spectral slope and CDOM absorption coefficient, first presented in Polar Waters by Stedmon and Markager (2001), was used to differentiate between locally produced marine CDOM versus terrestrial input into the Greenland Sea. In our case, $S_{300-650}$ and $a_{CDOM}(375)$ at high salinity partially follows the model for marine CDOM (Stedmon and Markager, 2001), but otherwise resembles the relationship found in Hudson Bay (Granskog, 2012) known to also be dominated by terrigenous CDOM.

Based on Fig. 6a,b, we suggest that in summer there are predominantly two mixing patterns, where Surface water of the White Sea Basin (SWB) mixes either with Barents Sea water (BSW) or with underlying Deep water (DW). We calculated theoretical conservative mixing lines between these water masses following the approach of Stedmon and Markager (2003). The following end-members were chosen: a) freshest samples from the upper layer in the White Sea (SWB end-member, average S = 19.469); b) deepest samples (> 100 m) in the White Sea basin (DW end-member, average S = 29.544); c) and samples from the core of Barents Sea waters in the central part of Voronka section (BSW end-member, average S = 34.315). These theoretical mixing lines are shown on Fig. 7c,d as well as Fig. 8c. Slight deviations from theoretical lines can be explained by uncertainties in the definition of the end-members, especially of SWB at lower salinities.

Interesting to note is that the mixing line between BSW and SWB is distinctly different on Fig. 7c and d. Differences reflect that $s_{275-295}$ is dominated by terrestrial DOM signal, while $s_{300-650}$ at $a_{375} < 2\ m^{-1}$ is diluted and actually show signatures of marine DOM, which is captured by $s_{300-650}$. Thus, distribution in $s_{300-650}$ values on Fig. 7d can also be explained by different quality of marine CDOM, with lower $S_{300-650}$ corresponding to fresh marine DOM, and higher $S_{300-650}$ values corresponding to older marine CDOM. The demonstrated theoretical mixing lines help to better understand mixing processes in the area of study and give support to conservative mixing of CDOM between the White Sea and Barents Sea waters.

A strong linear correlation between salinity and DOC (Fig. 8a) results in a zero-salinity estimate of $959 \pm 53\ \mu mol\ l^{-1}$ (Table 2), which is lower than previously reported values for the Northern Dvina of $1675\ \mu mol\ l^{-1}$ ($20.1\ mg\ l^{-1}$) (Gordeev et al., 1996). However, this estimate exceeds the flow-weighted DOC concentrations of six major Arctic rivers (Ob', Yenisei, Lena, Kolyma, Yukon, and Mackenzie) reported by Cooper et al. (2008). Among those rivers, Lena has the highest flow-weighted DOC concentration $762 \pm 63\ \mu mol\ l^{-1}$.

CDOM absorption or the spectral slope can potentially be used as a proxy for estimates of DOC content in coastal waters (e.g. Spencer et al., 2009). Relationships of $a_{CDOM}(350)$, $a_{CDOM}(300)$ and $a_{CDOM}(254)$ against DOC show a significant linear relationship in the White Sea (Fig. 8b; Table 2). The strongest linear relationship between CDOM absorption and DOC was found at shorter wavelengths ($a_{CDOM}(254)$), which has been previously highlighted in other coastal studies (e.g. Spencer et al., 2009; Asmala et al., 2012).

The spectral slope ratio S_R has low variability in the salinity range 20–33, and then a very rapid increase at higher salinities (Fig. 8c). The low variability in S_R at salinities below 33 indicates very little change in CDOM composition during mixing, generally follow theoretical conservative lines between SWB and BSW, and SWB and DW calculated after Stedmon and Markager (2003), which is in contrast to what was found in the Hudson Bay (Granskog, 2012). The increase of S_R at higher salinities indicates the mixing of terrestrial CDOM from the White Sea with CDOM from Barents Sea water. Largest spatial variability in S_R (not shown) was associated with waters originating from the Barents Sea, similar to $S_{275-295}$ (Fig. 3). Previously, S_R has been shown to be correlated to DOM molecular weight and has been previously used to distinguish between terrestrial and marine DOM signals (Helms et al., 2008). Higher ($S_R > 1$) values generally correspond to marine DOM with lower molecular weight, while lower ($S_R < 1$) values are associated with terrestrial DOM with higher molecular weight (Helms et al., 2008). High values ($S_R > 1$) were also associated with photochemical DOM decomposition and transformation (Helms et al., 2008; Granskog, 2012). In this study, S_R, generally ranged from 0.75 to 3.2 (Fig. 8c). Values of S_R below or around 1 were found in waters with salinity below 30–31 and DOC concentrations of 200–500 $\mu mol\ l^{-1}$. Values of S_R above 1 were found along the Voronka section, especially in its western part with corresponding DOC values below 100–150 $\mu mol\ l^{-1}$. Elevated S_R values indicate the influence of Barents Sea waters with DOM of marine origin (Hancke et al., 2014) but also aged and photochemically transformed CDOM transported to high latitudes with Atlantic waters. S_R above 4.5 were reported by Kowalczuk et al. (2013) in the centers of subtropical gyres in the Northern and Southern Atlantic Ocean. S_R found at lower salinities corresponds well to data from other Arctic studies. Stedmon et al. (2011) reported average values for major Arctic rivers in the range of 0.85–0.99, while thermokarst waters in Alaska were in the range 0.94 ± 0.07 (Cory et al., 2013). Spencer et al. (2009) reported S_R ratios for Yukon River in the range of 0.79–0.94, with lowest values found during the spring freshet, with a slight increase throughout the summer towards winter. Thus, based on S_R values surface waters of the White Sea basin contain predominantly CDOM of terrestrial origin, with possible compositional change within the basin presumably due to photochemical alteration, while Barents Sea waters found at Voronka section have autochtonous (marine) and photodegraded CDOM.

The fluorescence intensity ratio (Peak T:Peak C) shows that, there was almost 9 times more protein-like DOM in the Barents Sea waters compared to those impacted by terrestrial outflow (Fig. 8d). A 20 fold increase of the protein – like DOM component relative to terrestrial humic-like component was found by Guéguen et al. (2011) in the salinity gradient from riverine dominated estuaries toward the Arctic Ocean in the Hudson Bay and Hudson Strait. Lower salinity waters influenced by terrestrial DOM have high molecular weight ($S_R < 1$, Fig. 8c) and contain predominately polyaromatic water soluble organic compounds with corresponding high SUVA254 values of up to $3.7\ m^2\ g^{-1}$. The White Sea waters interfacing with Barents Sea at the Voronka Section contain DOM that is characterized by apparently low molecular weight ($S_R > 2$), possibly containing aliphatic water soluble organic compounds produced by phytoplankton, which is in line with observed high Peak T to Peak C ratio (up to 9.1) and low SUVA254 values (down to $1.0\ m^2\ g^{-1}$). The highest SUVA254 values and lowest Peak T to Peak C ratios were observed within freshest waters dominated by highest contribution of humic-like compounds (Fig. 8d). A closer look at changes of Peak T to Peak C ratio with salinity provide additional evidence about the dominance of terrestrial DOM in the White Sea opposed to Barents Sea waters dominated by marine DOM, and possible transformation in DOM characteristics during its transport from the White Sea into the adjacent Barents Sea.

5. Conclusion

The White Sea receives a considerable flux of freshwater and DOM from rivers. The characteristics of DOM from the inflowing Barents Sea waters contrast the riverine-influenced waters in the White Sea. Significant linear relationships between salinity and $\delta^{18}O$ across the White Sea indicated a dominant contribution of

riverine water to the freshwater budget and little evidence for influence of sea ice formation (brine rejection) or melt on surface waters. Similarly White Sea deep waters were devoid of significant brine additions from sea-ice formation, supporting the fact that winter cooling of Barents waters, and their strong tidally induced vertical mixing with White Sea waters in the Gorlo area are the likely source of the deep waters. The linear relationship between salinity and CDOM absorption and salinity and DOC concentrations suggests conservative mixing of DOM in the White Sea basin. However, deviations from the conservative mixing line exist at intermediate salinities and most likely indicate variability in freshwater end-member values between rivers discharging into the White Sea basin. A strong linear relationship between CDOM absorption and DOC provides a relatively easy tool to trace DOC using spectrophotometric measurements of CDOM absorption, thus providing a great potential for seasonal monitoring of DOM pool in the region, in situ as well as from satellites. There is clear evidence for export of terrestrial DOM and freshwater to the adjacent Barents Sea along the Eastern edge of the Voronka in surface waters. The limited changes in DOM characteristics within the White Sea suggests that the majority of DOM is exported unaltered to the adjacent Barents Sea and further to Siberian Shelf where it maybe be subjected to removal or entrained into halocline waters.

Acknowledgments

Authors thank the Northern Arctic Federal University, the Russian Geographic Society and other organizers of the "Floating University" cruise, as well as the crew of the RV Professor Molchanov. Vera Yavlovskaya, Ekaterina Bloshkina, Mikhail Makhotin, Vasiliy Bednenko helped with in situ water sample collection. Sergey Zhuravlev kindly helped to find river discharge data. Ocean Data View has been used for plotting (Schlitzer, 2015). We thank Heidemarie Kassens, Jens Hölemann, Irina Fedorova, Elena Dobrotina, Lyudmila Korolyeva, and Roman Vlasenkov for the help within the Otto Schmidt Laboratory (OSL, St. Petersburg, Russia). We thank Paul A. Dodd for valuable discussion. A.K.P., P.K. and M.A. G. were supported by the Polish–Norwegian Research Programme operated by the National Centre for Research and Development under the Norwegian Financial Mechanism 2009–2014 in the frame of Project contract Pol-Nor/197511/40/2013, CDOM-HEAT. For A.S. and A.K.P this study was partly supported by OSL fellowship grant 03PL043A, D1551. M.A.G. was supported by the Centre for Ice, Climate and Ecosystems (ICE) at the Norwegian Polar Institute. A.K.P. and B.V.I. were supported by the Roshydromet grant number 1.5.3.3 and President Grant MK-4049.2014.8. For B.V.I. funding was provided by Ministry of Education and Science of the Russian Federation, Project RFMEFI61014 × 0006, Agreement no. 14.610.21.0006 "Development of new methods and techniques for monitoring of hydrometeorological and geophysical state of Spitsbergen and Russian West Arctic." T.M. was supported by the EU Regional Development Foundation, Project 3.2.0801.12-0044. Finally, we thank two anonymous reviewers, who helped to improve the manuscript.

References

Alling, V., Sanchez-Garcia, L., Porcelli, D., Pugach, S., Vonk, J.E., vanDongen, B., Mörth, C.-M., Anderson, L.G., Sokolov, A., Andersson, P., Humborg, C., Semiletov, I., Gustafsson, Ö., 2010. Nonconservative behavior of dissolved organic carbon across the Laptev and east Siberian seas. Glob. Biogeochem. Cycles 24, 4.

Amon, R.M.W., Rinehart, A.J., Duan, S., Louchouarn, P., Prokushkin, A., Guggenberger, G., Bauch, D., Stedmon, C., Raymond, P.A., Holmes, R.M., McClelland, J.W., Peterson, B.J., Walker, S.A., Zhulidov, A.V., 2012. Dissolved organic matter sources in large Arctic rivers. Geochim. Cosmochim. Acta 94, 217–237.

Anderson, L.G., Amon, R., 2014. DOC in the Arctic Ocean. In: Hansell, Dennis A., Carlson, Craig A. (Eds.), Biogeochemistry of Marine Dissolved Organic Matter, 2nd ed.

Asmala, E., Stedmon, C.A., Thomas, D.N., 2012. Linking CDOM spectral absorption to dissolved organic carbon concentrations and loadings in boreal estuaries. Estuarine Coastal Shelf Sci. 111, 107–117.

Bauch, D., Dmitrenko, I.A., Wegner, C., Hölemann, J., Kirillov, S.A., Timokhov, L.A., Kassens, H., 2009. Exchange of Laptev Sea and Arctic Ocean halocline waters in response to atmospheric forcing. J. Geophys. Res.: Oceans (1978-2012) 114 (C5).

Belanger, S., Xie, H., Krotkov, N., Larouche, P., Vincent, W.F., Babin, M., 2006. Photomineralization of terrigenous dissolved organic matter in Arctic coastal Waters from 1979 to 2003: interannual variability and implications of climate change. Glob. Biogeochem. Cycles 20, 4.

Blough, N.V., Del Vecchio, R., 2002. Chromophoric DOM in the coastal environment. In: Hansell, D., Carlson, C. (Eds.), Biogeochemistry of Marine Dissolved Organic Matter. Academic Press, New York, pp. 509–546.

Bøsrheim, K.Y., Myklestad, S.M., 1997. Dynamics of DOC in the Norwegian Sea inferred from monthly profiles collected during 3 years at 66 N, 2 E. Deep Sea Res. Part I: Oceangr. Res. Pap. 44 (4), 593–601.

Cauwet, G., Sidorov, I., 1996. The biogeochemistry of Lena river: organic carbon and nutrients distribution. Mar. Chem. 53 (3), 211–227.

Cauwet, G., 1999. 15 Determination of dissolved organic carbon and nitrogen by high temperature combustion. In: Grasshoff, K., Kremling, K., Ehrhardt, M. (Eds.), Methods of Seawater Analysis. Wiley-VCH, Weinheim.

Coble, P.G., 1996. Characterization of marine and terrestrial DOM in seawater using excitation-emission matrix spectroscopy. Mar. Chem. 51 (4), 325–346.

Cooper, L.W., McClelland, J.W., Holmes, R.M., Raymond, P.A., Gibson, J.J., Guay, C.K., Peterson, B.J., 2008. Flow-weighted values of Runoff tracers (δ18O, DOC, Ba, alkalinity) from the six largest Arctic rivers. Geophys. Res. Lett. 35, 18.

Cory, R.M., Crump, B.C., Dobkowski, J.A., Kling, G.W., 2013. Surface exposure to sunlight stimulates CO2 release from permafrost soil carbon in the Arctic. Proc. Natl. Acad. Sci. 110 (9), 3429–3434.

Dodd, P.A., Rabe, B., Hansen, E., Falck, E., Mackensen, A., Rohling, E., Stedmon, C., Kristiansen, S., 2012. The freshwater composition of the Fram strait outflow derived from a decade of tracer measurements. J. Geophys. Res.: Oceans (1978–2012) 117 (C11).

Erickson III, D.J., Sulzberger, B., Zepp, R.G., Austin, A.T., 2015. Effects of stratospheric ozone depletion, solar UV radiation, and climate change on biogeochemical cycling: interactions and feedbacks. Photochem. Photobiol. Sci. 14 (1), 127–148.

Filatov, N., Pozdnyakov, D., Johannessen, O.M., Pettersson, L.H., Bobylev, L.P., 2007. White Sea: Its Marine Environment and Ecosystem Dynamics Influenced by Global Change. Springer Science & Business Media.

Findlay, H.S., Gibson, G., Kędra, M., Morata, N., Orchowska, M., Pavlov, A.K., Reigstad, M., Silyakova, A., Tremblay, J-É, Walczowski, W., Weydmann, A., Logvinova, C., 2015. Responses in Arctic marine carbon cycle processes: conceptual scenarios and implications for ecosystem function. Polar Res., 34.

Fransson, A., Chierici, M., Anderson, L.G., Bussmann, I., Kattner, G., Jones, E.P., Swift, J.H., 2001. The importance of shelf processes for the modification of chemical constituents in the waters of the Eurasian Arctic ocean: implication for carbon Fluxes. Cont. Shelf Res. 21 (3), 225–242.

Glukhovskiy, B. (Ed.), 1991. White Sea. Hydrometeorology and Hydrochemistry of USSR Seas Vol. 2. Hydrometeoizdat, Leningrad, p. 240.

Gordeev, V.V., Martin, J.M., Sidorov, I.S., Sidorova, M.V., 1996. A reassessment of the Eurasian river input of water, sediment, major elements, and nutrients to the Arctic ocean. Am. J. Sci. 296 (6), 664–691.

Granskog, M.A., Macdonald, R.W., Mundy, C.J., Barber, D.G., 2007. Distribution, characteristics and potential impacts of Chromophoric dissolved organic matter (CDOM) in Hudson strait and Hudson bay, Canada. Cont. Shelf Res. 27 (15), 2032–2050.

Granskog, M.A., Kuzyk, Z.Z.A., Azetsu-Scott, K., Macdonald, R.W., 2011. Distributions of Runoff , sea-ice melt and brine using δ18O and salinity data — a new View on freshwater cycling in Hudson bay. J. Mar. Syst. 88 (3), 362–374. http://dx.doi.org/10.1016/j.jmarsys.2011.03.011.

Granskog, M.A., 2012. Changes in spectral slopes of Colored dissolved organic matter absorption with mixing and removal in a terrestrially dominated marine system (Hudson bay, Canada). Mar. Chem. 134–135, 10–17. http://dx.doi.org/10.1016/j.marchem.2012.02.008.

Granskog, M.A., Stedmon, C.A., Dodd, P.A., Amon, R.M., Pavlov, A.K., Steur, L., Hansen, E., 2012. Characteristics of Colored dissolved organic matter (CDOM) in the Arctic outflow in the Fram strait: assessing the Changes and fate of terrigenous CDOM in the Arctic ocean. J. Geophys. Res.: Oceans (1978–2012) 117 (C12).

Granskog, M.A., Pavlov, A.K., Sagan, S., Kowalczuk, P., Raczkowska, A., Stedmon, C.A., 2015. Effect of sea-ice melt on inherent optical properties and vertical distribution of solar radiant heating in Arctic surface waters. J. Geophys. Res. Oceans 120, 7028–7039. http://dx.doi.org/10.1002/2014JC010632.

Guéguen, C., Granskog, M.A., McCullough, G., Barber, D.G., 2011. Characterisation of Colored dissolved organic matter in Hudson bay and Hudson strait using parallel factor analysis. J. Mar. Syst. 88, 423–433.

Hancke, K., Hovland, E.K., Volent, Z., Pettersen, R., Johnsen, G., Moline, M., Sakshaug, E., 2014. Optical properties of CDOM across the Polar Front in the Barents Sea: origin, distribution and significance. J. Mar. Syst. 130, 219–227.

Hansell, D.A., 2005. Dissolved organic carbon reference material program. Eos Trans. Am. Geophys. Union 86 (35), 318.

Helms, J.R., Stubbins, A., Ritchie, J.D., Minor, E.C., Kieber, D.J., Mopper, K., 2008. Absorption spectral slopes and slope ratios as indicators of molecular weight, source, and photobleaching of chromophoric dissolved organic matter. Limnol. Oceanogr. 53 (3), 955–969.
Hill, V.J., 2008. Impacts of Chromophoric Dissolved Organic Material on Surface Ocean Heating in the Chukchi Sea. J. Geophys. Res.: Oceans (1978–2012) 113.
Kattner, G., Lobbes, J.M., Fitznar, H.P., Engbrodt, R., Nöthig, E.M., Lara, R.J., 1999. Tracing dissolved organic substances and nutrients from the Lena river through Laptev Sea (Arctic). Mar. Chem. 65 (1), 25–39.
Kowalczuk, P., Tilstone, G.H., Zabłocka, M., Röttgers, R., Thomas, R., 2013. Composition of dissolved organic matter along an Atlantic meridional transect from fluorescence spectroscopy and parallel factor analysis. Mar. Chem. 157, 170–184.
McDougall, T.J., Barker, P.M., 2011. Getting started with TEOS-10 and the Gibbs seawater (GSW) oceanographic toolbox. SCOR/IAPSO WG 127, 1–28.
Murphy, K.R., Butler, K.D., Spencer, R.G.M., Stedmon, C.A., Boehme, J.R., Aiken, G.R., 2010. Measurement of dissolved organic matter fluorescence in aquatic environments: an interlaboratory comparison. Environ. Sci. Technol. 44, 9405–9412.
Lobbes, J.M., Fitznar, H.P., Kattner, G., 2000. Biogeochemical characteristics of dissolved and particulate organic matter in Russian rivers entering the Arctic Ocean. Geochim. Cosmochim. Acta 64 (17), 2973–2983.
Loeng, H., 1991. Features of the physical oceanographic conditions of the Barents Sea. Polar Res. 10 (1), 5–18.
Pavlov, A.K., Silyakova, A., Granskog, M.A., Bellerby, R.G., Engel, A., Schulz, K.G., Brussaard, C.P., 2014. Marine CDOM accumulation during a coastal Arctic *mesocosm* experiment: no response to elevated pCO2 levels. J. Geophys. Res.: Biogeosci. 119 (6), 1216–1230.
Pavlov, A.K., Granskog, M.A., Stedmon, C.A., Ivanov, B.V., Hudson, S.R., Falk-Petersen, S., 2015. Contrasting optical properties of surface waters across the fram strait and its potential biological implications. J. Mar. Syst. 143, 62–72.
Peralta-Ferriz, C., Woodgate., R.A., 2015. Seasonal and Interannual variability of pan-arctic surface mixed layer properties from 1979 to 2012 from hydrographic data, and the dominance of stratification for multiyear mixed layer shoaling. Prog. Oceangr. 134, 19–53. http://dx.doi.org/10.1016/j.pocean.2014.12.005.
Pokrovsky, O.S., Schott, J., Pokrovsky, G., 2000. Dissolved major and trace elements in two contrasting rivers and their estuarine zones of the White Sea (Karelia, Russia). Goldschmidt 2000. J. Conf. Abstr. 5 (2), 808.
Schlitzer, R., 2015. Ocean Data View, 〈http://odv.awi.de〉.
Serreze, M.C., Barrett, A.P., Slater, A.G., Woodgate, R.A., Aagaard, K., Lammers, R.B., Steele, M., Moritz, R., Meredith, M., Lee, C.M., 2006. The Large-scale freshwater cycle of the Arctic. J. Geophys. Res.: Oceans (1978–2012) 111 (C11).
Spencer, R.G., Aiken, G.R., Butler, K.D., Dornblaser, M.M., Striegl, R.G., Hernes, P.J., 2009. Utilizing chromophoric dissolved organic matter measurements to derive export and reactivity of dissolved organic carbon exported to the Arctic Ocean: a case study of the Yukon river, Alaska. Geophys. Res. Lett. 36, 6.
Stedmon, C.A., Markager, S., 2001. The optics of chromophoric dissolved organic matter (CDOM) in the Greenland Sea: an algorithm for differentiation between marine and terrestrially derived organic matter. Limnol. Oceanogr. 46, 2087–2093.
Stedmon, C.A., Markager, S., 2003. Behaviour of the optical properties of coloured dissolved organic matter under conservative mixing. Estuarine Coastal Shelf Sci. 57, 973–979.
Stedmon, C.A., Amon, R.M.W., Rinehart, A.J., Walker, S.A., 2011. The supply and characteristics of Colored dissolved organic matter (CDOM) in the Arctic Ocean: pan Arctic trends and differences. Mar. Chem. 124 (1), 108–118.
Stedmon, C.A., Granskog, M., Dodd, P.A., 2015. An approach to estimate the freshwater contribution from glacial melt and precipitation in east Greenland shelf waters using colored dissolved organic matter (CDOM). J. Geophys. Res.: Oceans 120, 1107–1117. http://dx.doi.org/10.1002/2014JC010501.
Stedmon, C.A., Markager, S., Kaas, H., 2000. Optical properties and signatures of Chromophoric dissolved organic matter (CDOM) in Danish coastal waters. Estuarine Coastal Shelf Sci. 51, 267–278.
Stein, R., Macdonald, R.W., 2004. Organic carbon budget: Arctic Ocean vs. Global Ocean, The Organic Carbon Cycle in the Arctic Ocean. Springer, Berlin Heidelberg, pp. 315–322.
Weishaar, J.L., Aiken, G.R., Bergamaschi, B.A., Fram, M.S., Fujii, R., Mopper, K., 2003. Evaluation of specific ultraviolet absorbance as an indicator of the chemical composition and reactivity of dissolved organic carbon. Environ. Sci. Technol. 37 (20), 4702–4708.
Xie, H., Bélanger, S., Song, G., Benner, R., Taalba, A., Blais, M., Tremblay, J-É, Babin, M., 2012. Photoproduction of ammonium in the Southeastern Beaufort Sea and its biogeochemical implications. Biogeosciences 9 (8), 3047–3061.